

## An Optimum Selection of Dual Coding Subfield Pattern for Plasma Displays

**Dong-Chan Kwak and Choon-Woo Kim**

**Imaging Systems Laboratory, Graduate School of Information Technology  
and Telecommunication, Inha University, Incheon, Korea**

E-mail: [cwkim@inha.ac.kr](mailto:cwkim@inha.ac.kr)

### Abstract

*Dual coding technique is one of the popular techniques to reduce the dynamic false contours on PDP. Subfield pattern is a key factor affecting the performance of dual coding technique. In this paper, an optimum subfield selection method based on genetic algorithm is proposed. Two types of string structures are defined to account for all the possible configurations of the dual coding subfield patterns. Genetic operators are proposed for optimization of dual coding subfield pattern. Quantitative measures to describe degrees of dynamic false contours and checkerboard patterns are defined. Experimental results indicate that dual coding subfield pattern that is determined by proposed method reduces dynamic false contours and checkerboard patterns.*

### 1. Introduction

Plasma display panel (PDP) represents gray levels by the pulse number modulation technique that results in undesirable dynamic false contours. The dynamic false contours appear on the smooth area of moving images. Various techniques have been proposed to reduce the dynamic false contours. They include the optimization of subfield pattern[1,2], equalizing pulse technique[3], the error diffusion, dithering[4-5], and dual coding technique[6].

Among these dynamic false contour reduction techniques, this paper is focused on the dual coding subfield optimization[6]. For the dual coding technique, a subfield of symmetrical shape is selected first. Types of subfield patterns can be divided into V, W, M, VVV and  $\Lambda\Lambda\Lambda$  shapes. Two different coding schemes are determined for a selected subfield pattern. Two different coding are applied alternatively, frame by frame, pixel by pixel or both. It has been reported that the dual coding technique can reduce the dynamic false contours[6]. However, it may result in undesirable checkerboard patterns. Performance of dual coding technique is determined by the subfield pattern and coding schemes. Selection of subfield pattern has been

made by trial and error or based on expert's experience.

In this paper, a systematic way of determining an optimum subfield pattern for dual coding technique is proposed. It is obtained by simultaneously minimizing quantified measures of the dynamic false contours and checkerboard patterns. As an optimization tool, genetic algorithm is employed. Two types of string structures are defined to account for all the possible configurations of the dual coding subfields, V, W, M, VVV and  $\Lambda\Lambda\Lambda$  shapes. Genetic operators are proposed for optimization. Quantitative measures to describe degrees of dynamic false contours and checkerboard patterns are proposed. Also, unified criterion combining two quantified measures is defined.

In section 2, the proposed method is explained in details. In section 3, the experimental results are presented.

### 2. Proposed Method of Selecting Optimum Dual Coding Subfield Pattern

Block diagram of the proposed method is shown in Figure 1. Each step of procedures shown in Figure 1 will be explained in detail. In this paper, various dual coding subfield patterns are divided into two groups. The first group represents subfield patterns whose smallest weight is located in the middle. Subfield patterns with the shapes of V, VVV, and M fall into this group. The second group contains subfield patterns whose largest weight is located in the middle. Subfield patterns of W and  $\Lambda\Lambda\Lambda$  shapes are classified into this group. In this paper, the first and second groups of subfield patterns are called as Type V and Type W subfield patterns, respectively.

The procedure shown in Figure 1 is independently applied to both of Type V and W subfields. Results of genetic algorithms for Type V and W are merged together. Optimum subfield pattern is selected from the merged set of subfield patterns.

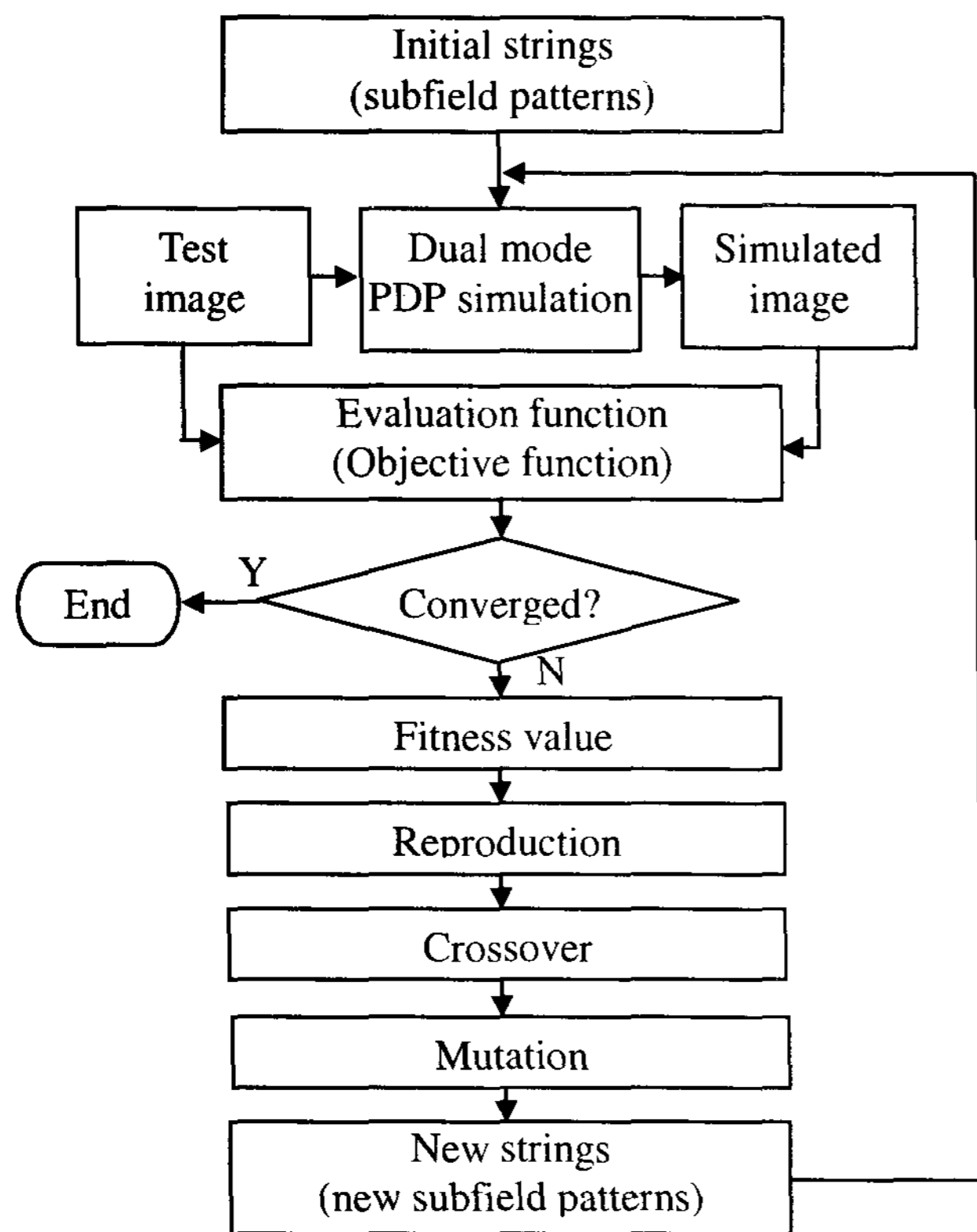


Figure 1. Block diagram of proposed method.

## 2.1. Structure of String

String for genetic algorithm in this paper represents subfield pattern. Let  $[sf(1) sf(2) sf(3) \dots sf(N-1), sf(N)]$  represent a subfield pattern with  $N$  weights and be arranged in ascending order. In case of 8 bits per pixel, they should satisfy the following equations.

$$\sum_{i=1}^N sf(i) = 255 \quad (1)$$

$$sf(n+1) \leq \left\{ \sum_{i=1}^n sf(i) \right\} + 1, n = 1, 2, \dots, N-1 \quad (2)$$

$$sf(1) = 1 \quad (3)$$

where  $N$  is the number of weights. Eq. (1-3) are sufficient conditions for single coding subfield pattern. However, additional requirements are needed for dual coding technique. Additional requirements vary according to the number of weights and configurations of subfield patterns. They are explained next.

For Type V subfield pattern, additional conditions are defined as follows.

$$10 \text{ subfield case } (N=10):$$

$$sf(2n-1) = sf(2n), n = 3, 4, 5 \quad (4)$$

$$11 \text{ subfield case } (N=11):$$

$$sf(2n) = sf(2n+1), n = 2, 3, 4, 5 \quad (5)$$

Additional conditions for Type W subfield are defined as follows.

$$10 \text{ subfield case } (N=10):$$

$$sf(2n) = sf(2n+1), n = 2, 3, 4 \quad (6)$$

$$sf(10) = sf(6) = sf(7) \quad (7)$$

$$\text{or } sf(10) = sf(8) = sf(9)$$

$$11 \text{ subfield case } (N=11):$$

$$sf(2n-1) = sf(2n), n = 3, 4, 5 \quad (8)$$

$$sf(11) = sf(7) = sf(8) \quad (9)$$

$$\text{or } sf(11) = sf(9) = sf(10)$$

Eq. (4-9) describe additional conditions for 10 and 11 subfields. When different number of weights is applied, similar conditions as in Eq. (4-9) can be defined. For a fixed number of subfields, additional conditions depend on the configuration of subfield pattern. That is why the proposed procedure in Figure 1 is independently applied to Type V and W.

Strings satisfying the above conditions are generated randomly for initial population. Initial population consists of subfield patterns with V or W configurations. It should be noted the other configurations such as the M, VVV and  $\Lambda\Lambda\Lambda$  shapes would be generated during genetic operations.

## 2.2. Test Image and PDP Simulation

Test image utilized in this paper is given in Figure 2. It is of size  $2 \times 512$ . For each of strings in population, PDP simulation[7] is applied. Before the PDP simulation, the order of subfields  $[sf(1) sf(2) sf(3) \dots sf(N-1), sf(N)]$  needs to be transformed. Transformation of subfield pattern for 10 and 11 subfields are given as follows.

10 subfield case ( $N=10$ )

Type V subfield :

$$[sf9 sf7 sf5 sf3 sf1 sf2 sf4 sf6 sf8 sf10] \quad (10)$$

Type W subfield :

$$[sf8 sf6 sf4 sf2 sf1 sf10 sf3 sf5 sf7 sf9] \quad (11)$$

11 subfield case ( $N=11$ )

Type V subfield :

$$[sf10 sf8 sf6 sf4 sf2 sf1 sf3 sf5 sf7 sf9 sf11] \quad (12)$$

Type W subfield :

$$[sf9 sf7 sf5 sf3 sf1 sf11 sf2 sf4 sf6 sf8 sf10] \quad (13)$$

PDP simulation is applied with predetermined dual codes and motion vector. Two different coding are alternatively applied pixel by pixel. Simulated images would exhibit different degrees of the dynamic false contours and checkerboard patterns. When population is made of  $M$  strings, simulation process generates  $M$  simulated images.

1	2	3	...	254	255	254	...	3	2	1
1	2	3	...	254	255	254	...	3	2	1

Figure 2. Test image.

### 2.3 Evaluation Function

Objective of genetic operation is to select a subfield pattern that simultaneously minimize the dynamic false contours and checkerboard patterns. Thus, an evaluation function for reproduction should account for degrees of the dynamic false contours and checkerboard patterns appeared on the simulated image. For a pair of the test and simulated image, quantified measures for dynamic false contour,  $E_{DFC}$ , and checkerboard pattern,  $E_{CHK}$ , are calculated.

Figure 3 shows a block diagram for calculation of  $E_{DFC}$  and  $E_{CHK}$ . For the calculation of  $E_{DFC}$ , both of the gamma corrected test image and simulated image are low passed. After Weber's law is applied, difference image is obtained and thresholded. A squared mean is calculated and serves as  $E_{DFC}$ . Calculation of  $E_{CHK}$  is explained next. After Weber's law is applied to both of the gamma corrected test image and simulated image, difference between two images is calculated. False contour regions are excluded and  $E_{CHK}$  is calculated by the following equation.

$$E_{CHK} = \frac{1}{PQ} \sum_{i=0}^{P-1} \sum_{j=0}^{Q-1} check^2(i, j) \quad (14)$$

where P and Q represent width and length of image and  $check(i, j)$  is defined as

$$check(i, j) = |A(i, j) - A(i, j + 1)| + |A(i, j) - A(i + 1, j)| - |A(i, j) - A(i + 1, j + 1)| \quad (15)$$

where  $A(i, j)$  is  $(i, j)$ th pixel of the difference image.

Suppose  $E_{DFC}(k)$  and  $E_{CHK}(k)$  be the calculated measures for  $k$ th string of population. An unified measure  $eval(k)$  is calculated by the following Eq. (16) and serves as a value of evaluation function for  $k$ th string.

$$eval(k) = \left( \frac{E_{DFC}(k) - E_{Min\_DFC}}{E_{Max\_DFC} - E_{Min\_DFC}} \right)^2 + \left( \frac{E_{CHK}(k) - E_{Min\_CHK}}{E_{Max\_CHK} - E_{Min\_CHK}} \right)^2 + C \quad (16)$$

where  $E_{Max\_DFC}$  and  $E_{Min\_DFC}$  are the maximum and minimum of  $E_{DFC}(k)$ ,  $k=1,2,\dots,M$ , respectively.  $E_{Max\_CHK}$  and  $E_{Min\_CHK}$  are the maximum and minimum of  $E_{CHK}(k)$ ,  $k=1,2,\dots,M$ , respectively.  $C$  is a positive constant.

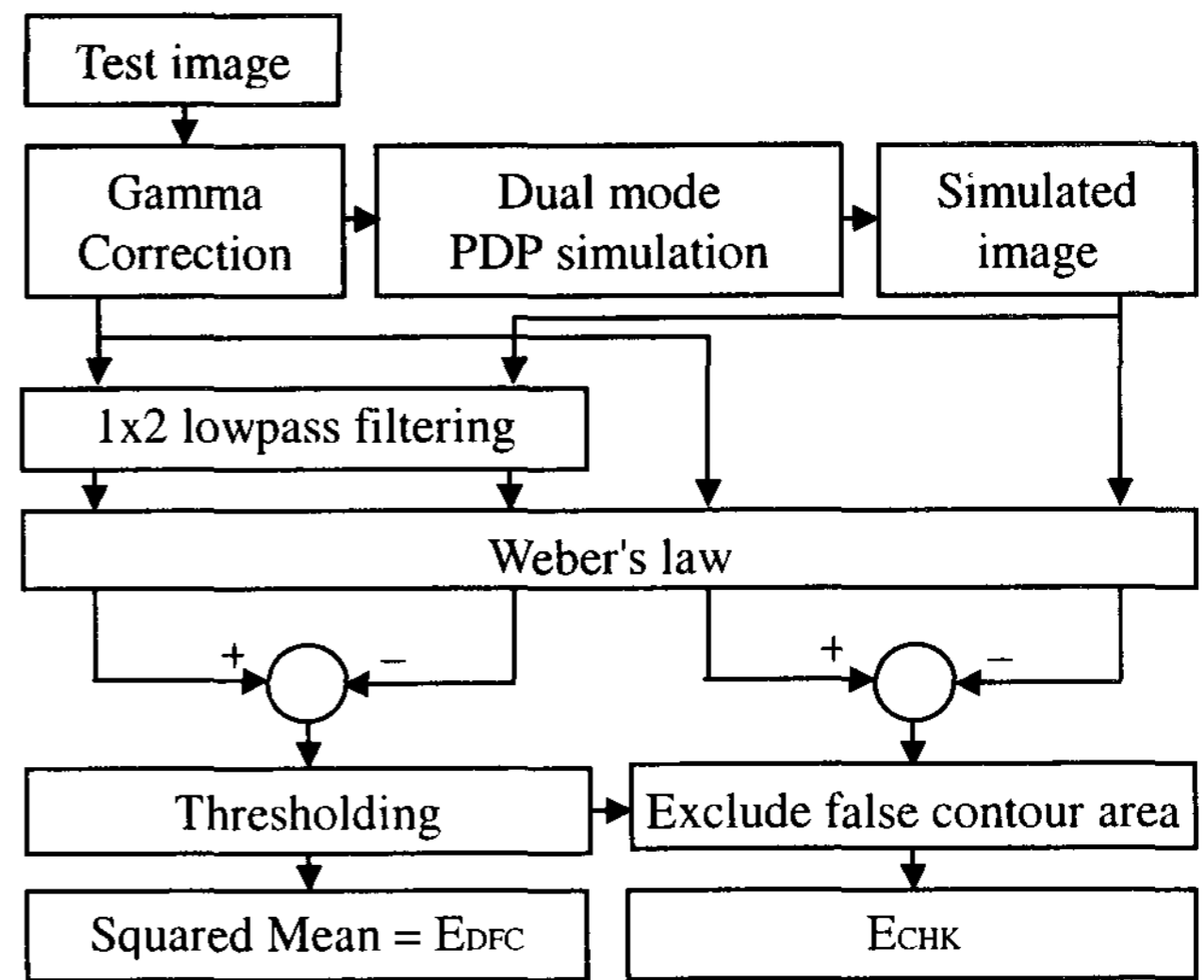


Figure 3. Block diagram for calculation of evaluation function

### 2.4 GA Operators

Genetic operations are applied to strings arranged in the form of  $[sf(1) sf(2) sf(3) \dots sf(N-1), sf(N)]$ . Fitness value of the  $k$ th string is calculated by

$$fitness\_value(k) = \frac{1}{eval(k)} \quad (17)$$

Reproduction probability of the  $k$ th string for next generation is calculated by Eq. (18).

$$prob(k) = \frac{fitness\_value(k)}{\sum_{i=0}^M fitness\_value(i)} \quad (18)$$

Crossover combines features of two parent strings to form two offspring. It is applied from the 2<sup>nd</sup> iteration of the loop shown in Figure 1. Crossover is achieved by trading the order of weights in predetermined position within the string. Selection of position for cross operation depends on Type of strings and number of subfields. It is explained next. For a given Type and number of subfields, two locations are selected which will serve as starting and ending points for the crossover operation. Candidates for such selection of locations are given as follows.

Type V subfield

10 subfield case (N=10):

$$position = sf(2n - 1), n = 1,2,3,4,5$$

11 subfield case (N=11):

$$position = sf(2n), n = 1,2,3,4,5$$

Type W subfield

10 subfield case (N=10):

$$position = sf(2n), n = 1,2,3,4$$

11 subfield case (N=11):

$$\text{position} = sf(2n-1), n = 1,2,3,4,5$$

Mutation is applied from the 1<sup>st</sup> iteration of the loop shown in Figure 1. Two types of mutation are applied in this paper. One is to change orders of weights. Suppose  $sf(m)$  and  $sf(l)$  are locations selected by the same procedure as in crossover. Weights  $sf(m)$  and  $sf(m+1)$  are exchanged with  $sf(l)$  and  $sf(l+1)$ , respectively. Second is to add/subtract a constant values to/from the weights in the predetermined positions. In addition to the initial population consisting of V and W shape subfields, subfields in M, VVV and  $\Delta\Delta\Delta$  shapes will be generated during iterations by the crossover and mutation.

After reproduction, mutation and crossover are applied. It is repeated until stopping criterion is satisfied. As mentioned, this procedure is independently applied to Type V and W subfields. Results for Type V and W are merged together. The optimum subfield pattern is selected from the merged set of subfield patterns.

### 3. Experimental Results

In the experiment, number of strings in initial population is 100 and number of iterations in genetic algorithm is 200. In order to examine whether the proposed technique finds global minimum without falling into local minima, exhaustive search for V-shaped subfield patterns has been performed. The number of V-shaped subfield patterns representing 256 gray levels with 11 subfield is 2827. For comparison, the proposed technique is applied to select the optimum subfield pattern of V-shape. The result of exhaustive search agrees with the result of the proposed method.

When representing 256 gray levels by 11 subfields, the optimum subfield pattern selected by the proposed method is [47 2 46 23 8 1 8 23 46 4 47]. Figure 4 shows the simulation result of an egg image. Figure 5 shows the simulation result for the gray ramp image. Vertical axis in Figure 5 represents the gray level differences between two consecutive pixels.

### 4. Conclusion

A systematic approach for optimum selection of subfield pattern for dual coding technique is proposed in this paper. The optimal dual coding subfield pattern is determined by minimizing the unified measure of the dynamic false contours and checkerboard patterns. For Type V, result of exhaustive search agrees with the result of the

proposed method. Experimental results indicate that the dual coding subfield pattern determined by proposed method reduces the dynamic false contours and checkerboard patterns.

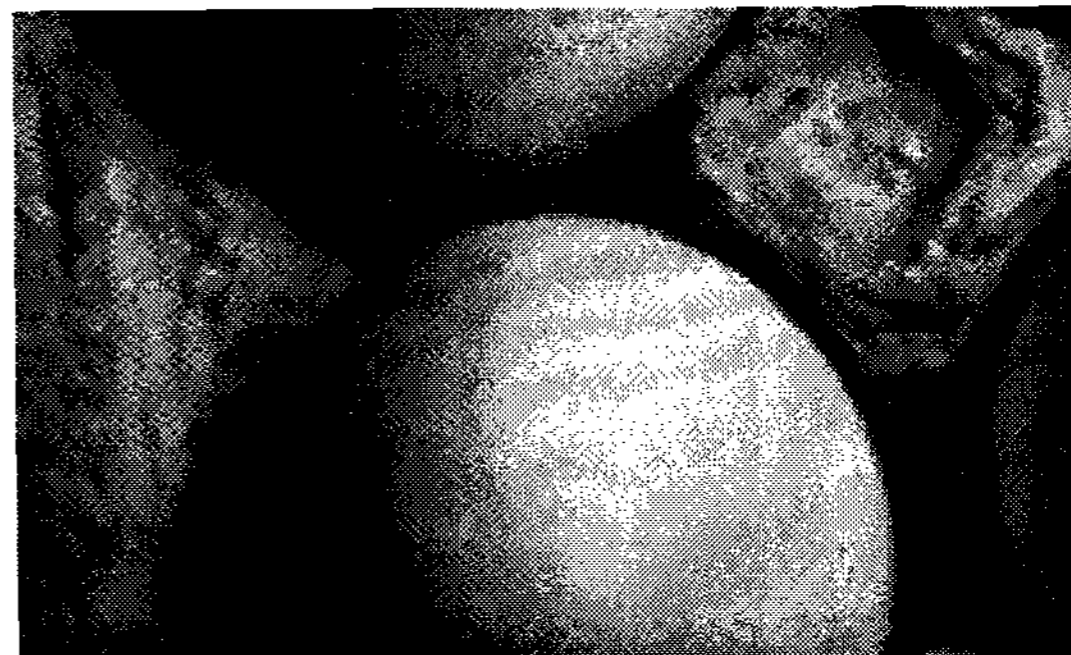


Figure 4. Simulation Result for 256 levels with 11 subfields [47 2 46 23 8 1 8 23 46 4 47]

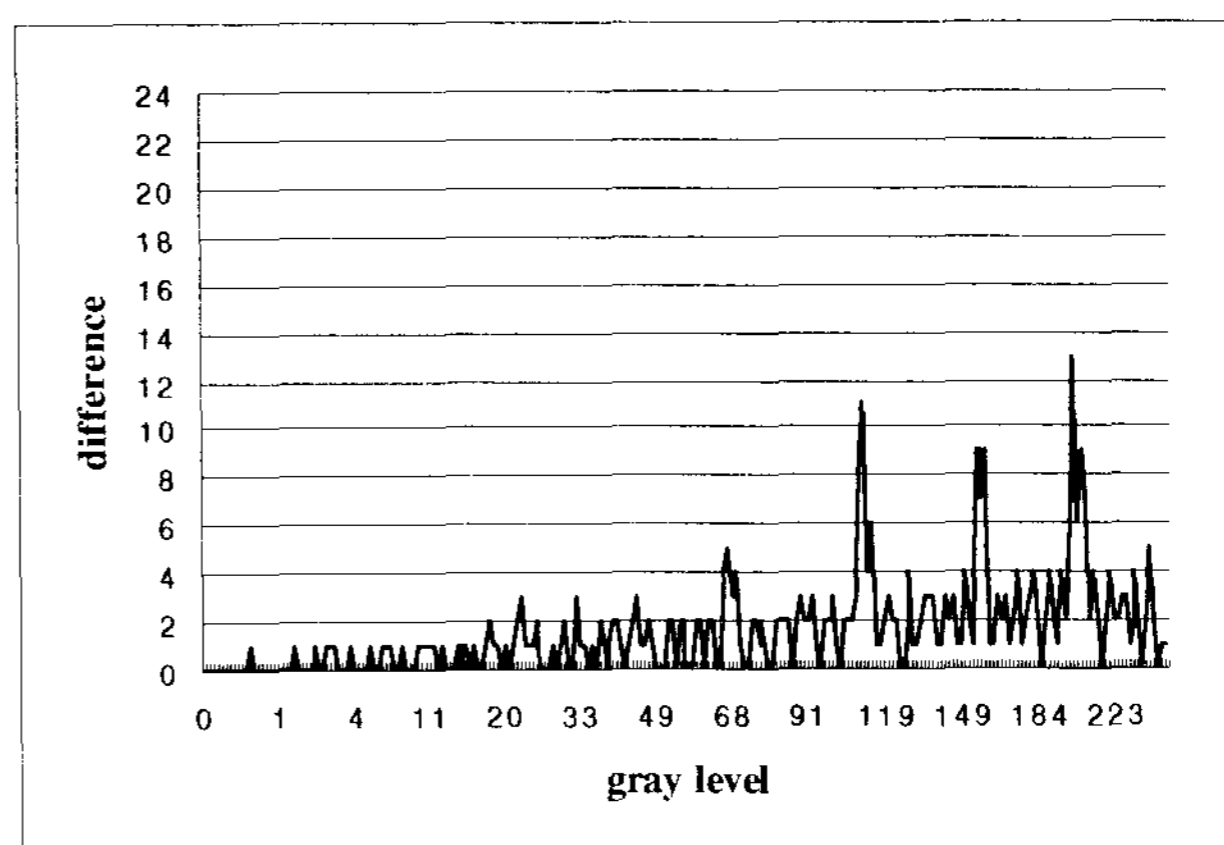


Figure 5. Result for Ramp Image : 256 levels with 11 subfields [47 2 46 23 8 1 8 23 46 4 47]

### 5. References

- [1] D. Zhu and T. Leacock, U.S. Patent 5,841,413
- [2] S. Park and C. Kim, "An Optimum Selection of Subfield Pattern for Plasma Displays Based on Genetic Algorithm", IEICE Trans. on Electronics, Vol. E84C, No. 11, pp. 1659-1666, Nov. 2001.
- [3] K.Toda et. al., "An Equalizing Pulse Technoque for Reducing Gray Scale Disturbances of PDPs Below the Minimum Visual Perception Level", Euro Display'96, pp.39-42,1996.
- [4] I.Kawahara and K.Sekimoto, "Dynamic Gray-Scale Control to Reduce Motion Picture Disturbance for High Resolution PDP", SID'99, pp.166-169
- [5] T.Tokunaga et. al., "Development of New Driving Method for AC-PDPs", IDW'99, pp.787-790, 1999.
- [6] M.Tajima et. al., U.S. Patent 6,222,512
- [7] I.Kawahara and K.Wani, "Simulation of motion picture disturbance for AC-PDP modeling virtual pixel on retina", IEICE Trans. on Electronics, Vol.E81-C, No.11, pp.1733-1739, Nov.1998.